

Mathematical Modeling of Particle Segregation During Centrifugal Casting of Metal Matrix Composites

B. Balout and J. Litwin

(Submitted August 6, 2009; in revised form September 7, 2010)

When a metal matrix composite undergoes centrifugal casting, the velocity, deceleration, displacement, and segregation of its particles are modeled according to changes in the centrifugal radius, as well as by variations in the molten metal viscosity as the temperature decreases during the cooling process. A cast aluminum alloy A356 reinforced by 10 V% of silicon carbide particles (SiC), with a median diameter of 12 μm , was used to conduct the experiments, and a mathematical modeling showed that the particles' volume fraction on the outer casting face varied according to whether the viscosity of the liquid metal used was constant or variable. If variations in viscosity during the cooling process are taken into account, then the volume fraction of the particles for a given time of centrifugation changes on the outer casting face, while it increases if the viscosity was constant. Modeling the particle segregation with variable viscosity produces results that are closer to those obtained with experiments than is the case when a constant viscosity is used. In fact, the higher the initial pouring and mold temperatures, the higher the effect of the viscosity variation on particle segregation.

Keywords centrifugal casting, metal matrix composite, particle segregation

1. Introduction

Centrifugal casting is a technology that relies on a centrifugal force to produce hollow and axisymmetric parts (cylinders, pipes, etc.). The technique is an effective method for the casting of particles' reinforced metal matrix composites (CMMp). The distribution of particles at the critical points of the section can be carried out by centrifugation. The centrifugal casting of CMMp allows the production of high-strength and light parts with very acceptable microstructures, and that are almost free of porosities, while being fairly compatible with the other parts in service.

The movement of the particles in a liquid matrix was studied to establish a method for controlling their concentration and distribution in a functionally graded composite (Ref 1). However, to simplify analysis, and because determining the solidification time and temperature distribution during the centrifugation process is a complicated problem, the authors considered the metal to be a liquid, thus obeying the Stokes law (constant temperature and viscosity). The authors thus found that the displacement of the particles toward the outer casting face ($\rho_P > \rho_l$) increases with an increase in the rotation speed and particle size. Moreover, it was noted that when the temperature of the mold and the metal is elevated, the metal

becomes less viscous, and the desired distribution of the reinforcing particles along the part section cannot be reached (Ref 2). In addition, the particles' size also influences their distribution inside the matrix. The zone rich in particles on the outer/inner faces increases with particle size, depending on the particle/matrix density ratio (Ref 3). On the other hand, under certain conditions, the particles close to the outer face are small in diameter, a phenomenon which is attributable to the solidification front, which tends to prevent large-size particles from moving freely toward the outer casting face (Ref 4).

According to Stokes law, for a laminar flow, the velocity of a particle in a liquid is constant and its acceleration is zero. However, during the centrifugation process, the centrifugal radius changes with the displacement of the particle and the melt viscosity increases during the cooling process. Thus, the particle velocity is not constant with time. Therefore, for optimal production using a functionally graded metal matrix composite, the centrifugation laws and the variation of the particle velocity through the matrix must be specified.

Several authors have studied the impact of centrifugation parameters, such as particle size and rotation speed, on the particles' segregation. However, the change in the particles' velocity with the change in the viscosity, along with its impact on their segregation, was not taken into account. Some authors have assumed that viscosity remains constant during particle segregation (Ref 5), while others, by studying the segregation of the particles during centrifugation in an Al/Si alloy, have assumed constant—but different—initial viscosities (Refs 6, 7). However, as mentioned by Lajoie and Suéry (Ref 6), change in viscosity as a function of temperature affects particle velocity and segregation, and, therefore, must be taken into account.

The primary goal of this article is to model, during centrifugation process, the particle segregation and volume fraction through the matrix and on the outer casting face while taking into account the change in the centrifugal radius combined with variations in viscosity as a function of time

B. Balout, Department of Mechanical Engineering, École de Technologie Supérieure, 1100 Notre-Dame Street West, (Corner Peel), Montreal, QC H3C 1K3, Canada; and **J. Litwin**, Cégep de Saint-Laurent, 625 Avenue Sainte-Croix, Montreal, QC H4L 3X7, Canada. Contact e-mails: bahaa.balout.1@ens.etsmtl.ca and bbalout@yahoo.ca.

List of symbols			
ω	Angular velocity, rad/s	$m_p^{A_i}$	Mass of the particles in an area A_i , g
γ	Acceleration, mm/s ²		
F_{net}	Net force on the particle, N	$m_T^{A_i}$	Total mass of the whole microstructure in an area A_i , g
F_{ω}	Centrifugal force, N		
F_{η}	Viscous force, N	$R_{M,i}$	Inner composite radius, mm
F_R	Repulsive force, N	$R_{M,e}$	Outer composite radius, mm
R_0	Particle position at time $t = 0$, mm	$R_{m,i}$	Inner mold radius, mm
d_p	Particle diameter, mm	$d_{m,e}$	Outer mold diameter, mm
R_p	Particle radius, mm	t_s	Solidification time, s
ρ_p	Particle density, kg/m ³	V_i	Sub-volume, mm ³
ρ_l	Liquid density, kg/m ³	L_i	Length, mm
η	Metal viscosity, Pa · s	h	Height, mm
η_e	Apparent viscosity, Pa · s	e	Thickness, mm
K_m	Thermal conductivity of the matrix, W/m · K	$fv_{V_i}^{t_0}$	Volume fraction of particles corresponding to the volume V_i at time $t = 0$, V%
V_p	Particle volume fraction, %V		
$v_p(t_i)$	Particle velocity at time t_i , mm/s	$fv_{V_i}^{t_s}$	Volume fraction of particles entering the sub volume V_i at time t_s , before the solidification begins on this volume, V%
$V_p(t_i \rightarrow t_i + \Delta t)$	Particle velocity at time interval ($t_i \rightarrow t_i + \Delta t$), mm/s		
V_c	Cooling rate, °C/s		
$a_i^{R_j}$	Particle acceleration as a function of time and position, mm/s ²	$fv_{V_i}^{t_s \rightarrow}$	Volume fraction of particles leaving the volume V_i at time t_s , V%
Q	Activation energy of viscous flow, kJ · mol ⁻¹		
R_g	Constant of perfect gases, J/K · mol	$fv_{V_i}^{t_s} \left(R_j - \Delta R/2 < R_{mi}^{t=0} + S_{(t_i)tot}^{R_j} < R_j \right)$	Volume fraction of particles moved to a sub volume V_i located between R_j and $R_j - \Delta R/2$ before the solidification begins, V%
Δt	Time increment, s		
$R_{t_i + \Delta t}$	Centrifugal radius at time $t_i + \Delta t$, mm	$fv_{V_i}^{t_s} \left(R_j < R_{mi}^{t=0} + S_{(t_i)tot}^{R_j} < R_j + \Delta R/2 \right)$	Volume fraction of particles moved to a sub volume V_i located between R_j and $R_j + \Delta R/2$ before the solidification begins, V%
R_{t_i}	Centrifugation radius at time t_i , mm		
t_i	Centrifugation time, s	$\Delta fv_{V_{i+1}}^{t_s} (s; fv_{(V_{i+1})} > 52\%)$	Excess of the particles' volume fraction of the sub volume V_{i+1} , V%
t_c	Cooling time, s		
C	Specific heat, J/kg · K ⁻¹		
H_f	Latent heat of fusion, J/kg	$R(fv)_j \Big _{j=0}^{t_s}$	Final position of particles' volume fraction before the solidification starts, mm
$T_{m,t_i}^{R_j}$	Temperature of liquid metal as a function of time and position, °C		
$T_{m,t_i + \Delta t}^{R_j}$	Molten metal temperature at time ($t_i + \Delta t$) and position R_j , °C	$R(fv)_j \Big _{j=0}^{t_0}$	Initial position of particles' volume fraction, mm
T_L, T_s	Liquidus and solidus temperatures, respectively, °C	$S_{(fv)R_j}^{t_i}$	Displacement of the particles' volume fraction located at an initial position (R_j) for a given time of centrifugation (t_i), before the solidification begins, mm
T_p	Overheated metal temperature, °C		
α	Coefficient		
Al	Aluminum	$v_{t_i}^{R_j}$	Velocity of particle located at an initial position (R_j) for a given time of centrifugation (t_i), mm/s
SiC	Silicon carbide		
A	Constant	ΔR	Radius increment, mm
m	Metal		
P	Particle		
c	Composite		
$C_p^{A_i} \Big _{i=0}^n$	Concentration of the particles in an area A_i , wt.%		

and position through the matrix. This will be done by modeling each physical parameter that affects the particle movement as the velocity, deceleration/acceleration, and displacement of the particles. This modeling enables an accurate measure of the particles' velocity and the prediction of their volume fraction on the outer casting face, knowing that an increase or decrease in the particle velocity affects the particles' segregation.

2. Experimental Conditions

The samples used to conduct the tests were provided in the form of Duralcan composite A356/SiC with a particle volume fraction and a median diameter of 10%V and 12 μ m, respectively. The experiments were conducted with different initial

metals and mold temperatures ($T_{\text{metal,in}} = 650, 680, \text{ and } 700 \text{ }^\circ\text{C}$, $T_{\text{mold,in}} = 30, 100, 350, \text{ and } 400 \text{ }^\circ\text{C}$).

A vertical centrifugal machine with an ordinary steel mold, 5 mm thick and 32 mm in diameter, with a layer of 100 μm thick hematite coating (Fe_2O_3) were used to conduct the experiments. The rotation speed used was 650 rpm.

Figure 1 shows the centrifugal casting system used to conduct the experiments.

The following dimensions are presented in Fig. 1:

$R_{M,i}$, $R_{M,e}$: the inner and outer composite radiuses, respectively (mm);

$R_{m,i}$, $d_{m,e}$: the inner mold radius and the outer mold diameter, respectively (mm).

The dimensions of the mold and the casting, as well as the parameters used and the composition of the alloy are presented in Table 1 and 2.

The themophysical properties of the matrix, particle, and mold are presented in Table 3, where ρ is the density, K is the thermal conductivity, C is the specific heat, H is the latent heat of fusion, T_L and T_s are the liquidus and solidus temperatures, respectively.

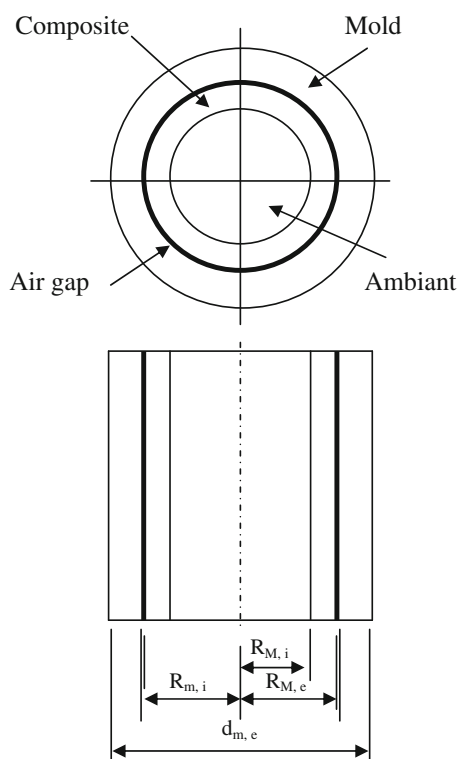


Fig. 1 Schematic representation of centrifugal casting system

The heat transfer coefficients by radiation and forced convection on the inner face metal/air and the outer face mold/air (Table 4) are calculated, based on Poirier and Poirier (Ref 8), taking into account the air properties, the boundary conditions, and the rotation speed.

The density and the specific heat of the composite are determined using the law of mixture, which takes into account the volume fraction of the ceramic particles.

The thermal conductivity of the composite was calculated based on the theory of effective middle EMT (Ref 9):

$$K = K_m(1 - V_p)/(1 + 0.5V_p) \quad (\text{Eq 1})$$

where K_m is the thermal conductivity of the matrix (W/m K) and V_p is the particle volume fraction.

To measure the concentration of the particles across the casting section and to analyze their distribution, photos of the microstructure were obtained with optical and scanning electron microscopes along the radial direction of the section. Each photo represents a distance of 125 μm from the outer face of the casting. The photos were printed, and the particles cut and separated from the matrix. The particles and the rest of the matrix were weighed together, and then separately, and the concentration of the particles calculated as the ratio between the particles mass and the total mass of the whole microstructure, as follows:

$$C_p^{A_i}|_{i=0}^n = \frac{m_p^{A_i}}{m_T^{A_i}} \times 100\% \quad (\text{Eq 2})$$

where $C_p^{A_i}|_{i=0}^n$ is the concentration of the particles in an area A_i , $m_p^{A_i}$ is the mass of the particles in an area A_i , and $m_T^{A_i}$ is the total mass of the whole microstructure in an area A_i .

3. Analysis and Modeling of Particle Velocity, Deceleration, Displacement, and Segregation During Cooling Process

The graduation degree of the particles and the variation of their distribution during centrifugation depend on several parameters, such as the density difference between the rein-

Table 1 Dimensions of the mold and the casting

Length, mm	Thickness, mm	Mass, kg	External radius, mm	Internal radius, mm
Casting				
62	3	0.1	32	29
Mold				
62	5		37	32

Table 2 Parameters used and composition of A356 aluminum alloy

Rotation speed, rpm	Initial mold temperature, $^\circ\text{C}$	Initial pouring temperature, $^\circ\text{C}$	Time increment (Δt), s					
650	30-100-350-400	650-680-700	0.005					
Composition of A356								
Si%	Mg%	Cu%	Ti%	Fe%	Zn%	Mn%	Others	Al%
6.5-7.5	0.3-0.45	≤ 0.2	≤ 0.2	≤ 0.15	≤ 0.1	≤ 0.1	≤ 0.15	Balance

Table 3 Thermophysical properties of aluminum A356, particles and steel mold

Thermophysical properties	Steel	A356	SiC	Composite A356/SiC
ρ , kg/m ³	7800	2400	3200	2480
K , W/m·K	42.2	151	24	130
C , J/kg·K	473	938	690	913
H_f , J/kg	...	389000
T_L , °C	...	612.8
T_{ss} , °C	...	557

Table 4 Heat transfer coefficients by forced convection and radiation

Metal temperature, °C	$h_{total,metal/air}$ W/m ² ·K
<i>Metal/air</i>	
650	107.27
680	107.72
700	108.01
Metal temperature, °C	$h_{total,mold/air}$ W/m ² ·K
<i>Mold/air</i>	
30	82.84
100	84.00
350	87.04
400	88.02

forcements and the matrix, the particle diameter, the melt viscosity, and the rotation speed.

Under a laminar flow, the particle velocity in a liquid is deduced from Stokes' law for a constant liquid temperature and viscosity, and under zero acceleration.

According to Raju and Mehrotra (Ref 3), during centrifugal casting, a particle which is suspended in the liquid is subjected to different forces, such as the centrifugal force, the viscous force, the repulsive force, and the gravitational force (Fig. 2). The centrifugal acceleration (γ) is much greater than the gravitational acceleration (g), and so the gravitational force and the vertical displacement of the particle can be ignored. Thus, the force balance equation on the particle can be expressed as:

$$F_\omega - F_\eta - F_R = F_{net} \quad (\text{Eq 3})$$

where F_{net} is the net force on the particle, F_ω is the centrifugal force, F_η is the viscous force, F_R is the repulsive force

The effect of the repulsive force on the particle is only significant if the particle is close to the solid-liquid interface. If the particle is not influenced by the solid-liquid interface, then the force balance can be expressed as (Ref 3):

$$F_\omega - F_\eta = F_{net} \quad (\text{Eq 4})$$

Equation 4 can be written as (Ref 3):

$$\frac{4}{3} \pi R_p^3 (\rho_p - \rho_l) \omega^2 R - 6\pi \eta R_p \frac{d_r}{dt} = \frac{4}{3} \pi R_p^3 \rho_p \frac{d^2 R}{dt^2} \quad (\text{Eq 5})$$

where R_p is the radius of the particle (mm), ω is the angular velocity (rad/s), R is the centrifugation radius (mm), ρ_p , ρ_l

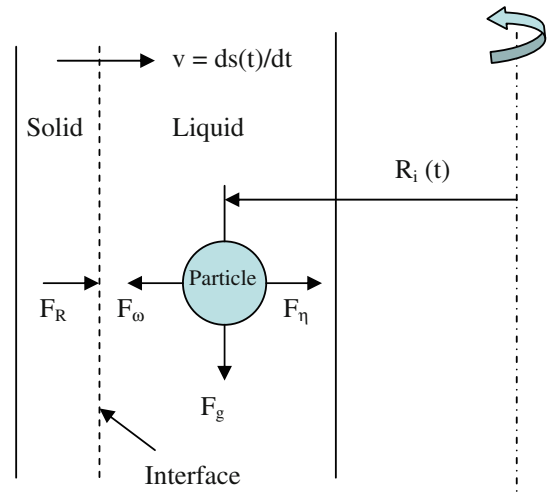


Fig. 2 Schematic representation of the forces acting on a moving particle in the melt (Ref 3)

are the particle and liquid densities, respectively (kg/m³), η is the melt viscosity (Pa·s).

Based on Eq 5, the velocity of a spherical particle which is moving in a liquid with zero acceleration is expressed as:

$$v_p = \frac{4\omega^2 \cdot R \cdot (\rho_p - \rho_l) \cdot R_p^2}{18\eta} \quad (\text{Eq 6})$$

Again based on Eq 5, for a particle moving with a constant velocity, the position of the particle at time t can be written as (Ref 3):

$$R(t) = R_0 \exp \left[\frac{4\omega^2 \cdot (\rho_p - \rho_l) \cdot R_p^2 \cdot t}{18\eta} \right] \quad (\text{Eq 7})$$

where R_0 is the position of the particle at time $t = 0$

When the liquid metal is overheated, the extraction of the superheat could last for a short or long time before the onset of solidification, depending on the initial pouring temperature, the molding conditions, and the cooling rate. On the other hand, the melt viscosity changes during cooling process as a function of time and position through the matrix. This variation of the viscosity as a function of temperature can be determined by the Arrhenius relation:

$$\eta = A \exp \left(\frac{Q}{R_g \cdot T_m} \right) \quad (\text{Eq 8})$$

where A is a constant, Q is the activation energy of viscous flow (kJ/mol), R_g is the constant of perfect gases ($R_g = 8.31441 \text{ J} \cdot \text{k}^{-1} \cdot \text{mol}^{-1}$), T_m is the absolute metal temperature (K).

The apparent melt viscosity also changes depending on the particle volume fraction, through the following equation (Ref 10):

$$\eta_c = \eta \cdot \alpha \quad (\text{Eq 9})$$

$$\alpha = 1 + 2.5 \cdot V_p(t) + 10.05 \cdot V_p^2(t) \quad (\text{Eq 10})$$

where η_c is the apparent melt viscosity (Pa·s), α is a coefficient, $V_p(t)$ is the volume fraction of particles as a function of time.

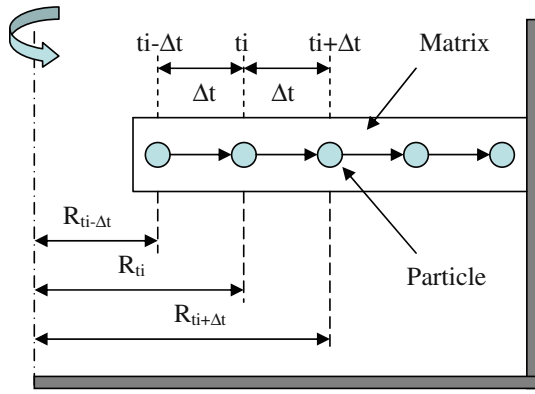


Fig. 3 Schematization of the centrifugal radius variation with time during the centrifugation process ($\rho_p > \rho_l$)

According to Stokes' law (Eq 6), the particle moves in the liquid with zero acceleration. Moreover, according to Eq 7, the particle position at any time (t) is calculated using a centrifugal radius corresponding to its position at time (t_0). However, the position of the particle at time (t) is influenced by the variation of the centrifugal radius during its displacement and the increase in the melt viscosity during the cooling process. The centrifugal radius between the rotation axis and the particle increases during the movement of the particle toward the outer face of the casting and decreases during its movement toward the inner face. This increase/decrease in the centrifugal radius generates an acceleration/deceleration of the particles during their displacements. Moreover, the temperature variation of the molten metal during the cooling process affects its viscosity. An increase or decrease in viscosity during the casting process may affect the velocity of the particles, and thereafter, their degree of graduation. Therefore, the final behavior of the particle is the result of the competition between the deceleration caused by the increase in the melt viscosity and the acceleration/deceleration caused by the change in the centrifugation radius. Thus, for the given experimental conditions, the centrifugal radius, the viscosity, and the velocity of the particle are not constant with time and position and must be taken into account when modeling the segregation of particles, as will be shown later in this study.

3.1 Modeling of Particle Velocity

Figure 3 schematizes the variation of the centrifugal radius with time for a particle which advances toward the outer face.

By combining Eqs 6, 8, 9, and 10, the particle velocity at each interval of time can be determined while taking into account the variation of the centrifugal radius and melt viscosity as a function of time interval and position through the matrix, through the following equation:

$$v_{p(t_i \rightarrow t_i + \Delta t)} = \frac{(\rho_p - \rho_l) \cdot d_p^2 \cdot \omega^2 \cdot R_{(t_i)}}{18 \cdot A \cdot \exp\left(\frac{Q}{R_E \cdot T_{m(t_i)}}\right) \cdot \alpha} \quad (\text{Eq 11})$$

The variation of the melt temperature and of the centrifugal radius can be expressed at each time interval, taking into account the position across the section, through the following equations:

$$T_{m(t_i + \Delta t)}^{R_j} = T_{m(t_i)}^{R_j} - v_{c(t_i)}^{R_j} \cdot \Delta t \quad (\text{Eq 12})$$

- Particle density smaller than that of liquid metal ($\rho_p < \rho_l$):

$$R_{t_i + \Delta t} = R_{t_i} - v_{p(t_i)} \cdot \Delta t \quad (\text{Eq 13})$$

- Particle density bigger than that of liquid metal ($\rho_p > \rho_l$):

$$R_{t_i + \Delta t} = R_{t_i} + v_{p(t_i)} \cdot \Delta t \quad (\text{Eq 14})$$

where $T_{m,t_i}^{R_j}$ is the melt temperature as a function of time and position through the matrix ($^{\circ}\text{C}$), $R_{t_i + \Delta t}$ is the centrifugal radius at time $t_i + \Delta t$ (mm), R_{t_i} is the centrifugal radius at time t_i (mm), $v_{p(t_i)}$ is the particle velocity at time t_i (mm/s), v_c is the cooling rate ($^{\circ}\text{C/s}$), Δt is the time increment (s).

The combination of Eqs 11, 12, and 14 allows us to discretize the particle velocity and to deduce its real variation across the casting section due to the increase in the centrifugal radius and melt viscosity. Furthermore, according to Stokes' law, the particle velocity is constant, and its acceleration is zero. In our study, these conditions are met because according to our modeling, the centrifugal radius and viscosity stay constant during the movement of the particle over a given small time interval (for example, from $t_i - \Delta t$ to t_i), which means that the velocity at which the particle moves in this time interval is constant and its acceleration is zero. The centrifugal radius and viscosity change and increase when switching to another time interval (for example, from t_i to $t_i + \Delta t$). In this new time interval, the velocity of the particle is influenced by another centrifugal radius and another viscosity value. Thus, the velocity of the particle changes, but remains constant with zero acceleration in this new time interval. Figure 12 and 13 in Appendix 1 shows the discretization and variation in the melt viscosity and particle velocity as a function of time for different time intervals and a given particle position. In these figures, a time increment (Δt) of 0.03 s was used to show clearly the invariance of the melt viscosity and particle velocity at each time interval. However, the modeling of the particle segregation was done with $\Delta t = 0.005$ s.

3.2 Modeling of Particle Acceleration/Deceleration

The average particle acceleration/deceleration as a function of time and position can be modeled taking into account the constant velocities of the particle at every two successive time intervals, through the following equations:

$$a = \frac{\partial v}{\partial t} \quad (\text{Eq 15})$$

$$\int_{v_1}^{v_2} dv = \int_{t_1}^{t_2} a \cdot dt \quad (\text{Eq 16})$$

$$a_{t_i}^{R_j} = \frac{v_{(t_i \rightarrow t_i + \Delta t)}^{R_j} - v_{(t_i - \Delta t \rightarrow t_i)}^{R_j}}{\Delta t} \quad (\text{Eq 17})$$

where R_j is the initial position of the particle from the rotation axis.

The average deceleration/acceleration of the particle is modeled based on the change of particle velocity between two successive intervals of time. Thus, the deceleration/acceleration of the particle between two successive time intervals is constant, and Stokes' law, which expresses the particle velocity with zero acceleration, is respected for each time interval during which the particle moves. The deceleration changes when

switching to two other successive time intervals. This is repeated for many time intervals until the temperature reaches the liquidus temperature of the metal, where the particle velocity is considered zero. Figure 14 in Appendix 1 shows the discretization and the variation of the particle deceleration as a function of time intervals.

3.3 Modeling of Particle Displacement

The distance travelled by the particle for a given position and time interval can be determined considering its velocity and acceleration/deceleration during the cooling process, as follows:

$$S = \int_{v_1}^{v_2} \frac{v}{a} \partial v \quad (\text{Eq 18})$$

$$S = \frac{v_2^2 - v_1^2}{2a} \quad (\text{Eq 19})$$

$$S_{t_i}^{R_j} = \frac{\left(v_{t_i \rightarrow t_i + \Delta t}^{R_j}\right)^2 - \left(v_{t_i - \Delta t \rightarrow t_i}^{R_j}\right)^2}{2a_{t_i}^{R_j}} \quad (\text{Eq 20})$$

The total distance travelled by the particle as a function of time and position through the matrix can be expressed as follows:

$$S_{\text{tot}}^{R_j} = \sum_{i,j=0}^n S_{t_i}^{R_j} = \sum_{i,j=0}^n \frac{\left(v_{t_i \rightarrow t_i + \Delta t}^{R_j}\right)^2 - \left(v_{t_i - \Delta t \rightarrow t_i}^{R_j}\right)^2}{2a_{t_i}^{R_j}} \quad (\text{Eq 21})$$

where S is the travelled distance (mm), R is the position from the rotation axis (mm), v is the particle velocity (mm/s), a is the acceleration (mm/s²)

In the modeling of the particle velocity, acceleration/deceleration, and displacement, the part thickness was divided into several sub-volumes. The distance from the rotation axis to the middle of each sub-volume (R_j) represents the initial position of the particle. Moreover, based on the work of Raju et al. (Ref 3, 6, 7), it was assumed that the particles are stopped by the liquid front, and that they move during the extraction of superheat before the temperature drops below liquidus. The influence of the movement of the particles on their segregation during solidification is assumed to be negligible. Thus, the maximum segregation of the particles on the outer/inner faces is produced during the cooling process before the solidification begins.

3.4 Modeling of Particle Segregation

In order to determine the maximum particle volume fraction on the outer casting face and their degree of graduation across the section during centrifugation, before the solidification begins, the casting thickness was divided into several sub-volumes (V_i) of length (L_i), height (h), and thickness (e), each containing an initial particle volume fraction of 10%V (Fig. 4). The final volume fraction of the particles was calculated in each sub-volume through Eq 22, taking into consideration the variation of the particle velocity due to the increase in viscosity and centrifugal radius as a function of time and position.

In the modeling, the variation of the particles' volume fraction with time was considered by ensuring the conservation of the total particles' volume fraction through the matrix at all

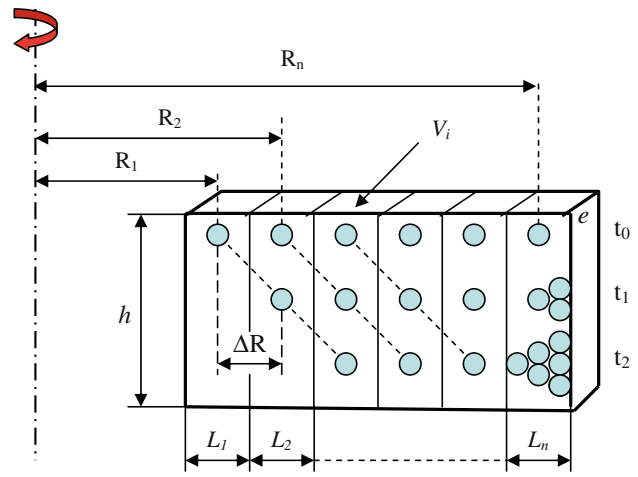


Fig. 4 Representation of particle displacement and segregation during centrifugation

times and, thus, by ensuring the conservation of the total mass at a given time. Thus, the modeling of the particles' segregation and of the changes in their volume fractions is based on the particles' movement and volume/mass conservation through the part section at any instant of time.

$$fV_{V_i}^{t_i} = fV_{V_i}^{t_0} + fV_{V_i}^{t_s} - fV_{V_i}^{t_s} + \sum_{i=0}^n \Delta fV_{V_{i+1}(fV_{i+1} > 52\%)}^{t_s} \quad (\text{Eq 22})$$

where

$$\begin{aligned} fV_{V_i}^{t_s} = & \left[\sum_{i,j=0}^n fV_{V_i}^{t_s} \left(R_j - \Delta R/2 < R_{(ini)}^{t=0} + S_{(t_i)tot}^{R_j} < R_j \right) \right] \\ & - \sum_{i,j=0}^n \frac{fV_{V_i}^{t_s}}{\Delta R} \cdot \left[R_j - \left(R_{(ini)}^{t=0} + S_{(t_i)tot}^{R_j} \right) \right] \\ & + \left[\sum_{i,j=0}^n fV_{V_i}^{t_s} \left(R_j < R_{(ini)}^{t=0} + S_{(t_i)tot}^{R_j} < R_j + \Delta R/2 \right) \right] \\ & - \sum_{i,j=0}^n \frac{fV_{V_i}^{t_s}}{\Delta R} \cdot \left[\left(R_{(ini)}^{t=0} + S_{(t_i)tot}^{R_j} \right) - R_j \right] \end{aligned} \quad (\text{Eq 23})$$

$$fV_{V_i}^{t_s} = \left(fV_{V_i}^{t_0} + \sum_{i=0}^n fV_{V_i}^{t_s} \right) \left(fV_{V_{i+1}}^{t_s} < 52\%, T_{V_{i+1}}^{t_s} \geq T_L \right) \quad (\text{Eq 24})$$

$$R(fV)_j \Big|_{j=0}^n = R(fv)_j \Big|_{j=0}^n + \sum_{i,j=0}^n S_{(fV)_{R_j}}^{t_i} \quad (\text{Eq 25})$$

where $fV_{V_i}^{t_0}$ is the volume fraction of particles corresponding to the volume V_i at time $t = 0$, $fV_{V_i}^{t_s}$ is the volume fraction of particles entering the sub volume V_i at time t_s , before the solidification begins on this volume, $fV_{V_i}^{t_s}$ is the volume fraction of particles leaving the sub volume V_i at time t_s , before the solidification begins on this volume, $fV_{V_i}^{t_s} \left(R_j - \Delta R/2 < R_{(ini)}^{t=0} + S_{(t_i)tot}^{R_j} < R_j \right)$ is the volume fraction of particles moved to a sub volume V_i located between R_j and $R_j - \Delta R/2$ before the solidification begins on this volume,

$f_j^{t_s}$ is the volume fraction of particles moved to a sub volume V_i located between R_j and $R_j + \Delta R/2$ before the solidification begins on this volume, $\Delta f_{V_{i+1}(f_{i+1}) > 52\%}$ is the excess of the particle volume fraction of the sub volume V_{i+1} , ΔR is the radius increment, $R(f_j)_{j=0}^{t_s}$ is the final position of the particle volume fraction, $R(f_j)_{j=0}^{t_0}$ is the initial position of the particle volume fraction at time $t = 0$, T_L is the liquidus temperature, $S_{(f_j)R_j}^{t_i}$ is the distance travelled by the particle volume fraction located at an initial position (R_j) for a given time of centrifugation (t_i), before the solidification begins, $v_{t_i}^{R_j}$ is the velocity of particle located at an initial position (R_j) for a given time of centrifugation (t_i), $a_{t_i}^{R_j}$ is the acceleration of particle located at an initial position (R_j) for a given time of centrifugation (t_i).

According to Watanabe et al. (Ref 1), the maximum volume fraction for the close packing of spherical particles in a composite is 74%V, and 52%V for a simple cubic packing of SiC.

4. Modeling of Cooling Rate

In our analysis, Cartesian co-ordinates were considered during the modeling of the cooling rate because of the small thickness of the part compared to its diameter. The heat transfer mechanism produced between the metal and the mold is a transient mechanism. The variation of the cooling rate and temperature as a function of time and position across the mold and metal sections were modeled through the implicit finite difference formulation using FLUENT for a transient one-dimensional unsteady state of solidification.

The variation of the cooling rate with time and position through the matrix can be expressed by the following equation:

$$v_{c,t_i}^{R_j} \Big|_{i,j=0}^n = \frac{T_p - T_{m,t_i}^{R_j}}{t_{c,i}} \quad (\text{Eq 26})$$

where $T_{m,t_i}^{R_j}$ is the metal temperature for given time and position ($^{\circ}\text{C}$), T_p is the temperature of superheated metal ($^{\circ}\text{C}$), t_c is the cooling time (s).

The modeling of the cooling/solidification on FLUENT takes into account the variation of the heat transfer coefficient mold/metal, as well as the contact resistance and the air gap formed between the mold and the metal as a result of the shrinkage of the latter during the solidification process. This is done using an additional heat transfer resistance mold/metal, with a liquid fraction less than 1 (Ref 11).

5. Results

The main purpose of this article is to show the influence of the increase in viscosity on the particle movement and volume fraction on the outer casting face while taking into account the change in the centrifugal radius during the particle displacement. As a first step, the influence of the change in the initial particle volume fraction on the apparent melt viscosity during centrifugation was not considered. Doing so allowed us to

determine the influence of the increase in viscosity on the particle velocity, acceleration/deceleration, and displacement due to the decrease in the temperature alone without it being influenced by other phenomena, such as changes in the particle volume fraction. Thereafter, the calculation of the particle volume fraction and segregation across the casting section is done with and without taking into account the influence of the variation in the particle volume fraction on the apparent melt viscosity and particle velocity and segregation across the casting section. This calculation allows us to clarify the influence of the increase in viscosity on the particle segregation across the casting section due to the decrease in temperature, on the one hand, and increase in the particle volume fraction, on the other.

In this modeling, the following assumptions were considered:

- The particles are spherical in shape;
- There is no clustering of the particles during their displacements;
- The particles are not rejected by the solidification front;
- The particles do not move in the mushy zone of the cast;
- There is no thermal resistance between particles and liquid metal;
- The vertical particle movement is neglected because of the high centrifugal force.

5.1 Cooling Rate, Temperature, and Viscosity

For a composite produced by centrifugal casting, the change in the rotation speed and in the initial pouring and mold temperatures change the cooling rate. Table 5 shows, for a given rotation speed and initial pouring and mold temperatures, the change in the cooling rate on the outer casting face as a function of time.

It can be seen (Table 5) that the cooling rate on the outer casting face decreases with the increase of cooling time due to the reduction of heat transfer at the metal/mold interface with time. Furthermore, it can be seen (Table 6) that during the extraction of superheat, the temperature on the outer casting face decreases as a function of time. On the other hand, the temperature on the mold inner face increases with time and starts decreasing by the end of the cooling time. Furthermore, during cooling, the liquid front advances from the outer to the inner casting face, while in the mold, the heat flow advances from the inner to the outer mold face. The change in the melt viscosity during cooling will therefore be influenced by the variation of the cooling rate and temperature on the outer casting face and through the matrix, as a function of time and position.

Table 5 Cooling rate as a function of time on the outer casting face ($T_{\text{metal,in}} = 700 \text{ }^{\circ}\text{C}$, $T_{\text{mold,in}} = 400 \text{ }^{\circ}\text{C}$)

Time, s	Position from the outer casting face: 0.1 mm Cooling rate, $^{\circ}\text{C/s}$
0.12	348
0.21	284
0.30	251
0.39	223
0.48	186
0.57	159

Table 6 Temperatures as a function of time on the outer and inner casting and mold faces, respectively ($T_{\text{metal,in}} = 700\text{ }^{\circ}\text{C}$, $T_{\text{mold,in}} = 400\text{ }^{\circ}\text{C}$)

Time, s	Temperature on the outer casting face, $^{\circ}\text{C}$	Temperature on the inner mold face, $^{\circ}\text{C}$
0	700	400
0.12	658	453
0.21	640	464
0.30	625	469
0.39	613	470
0.48	611	466
0.57	610	463

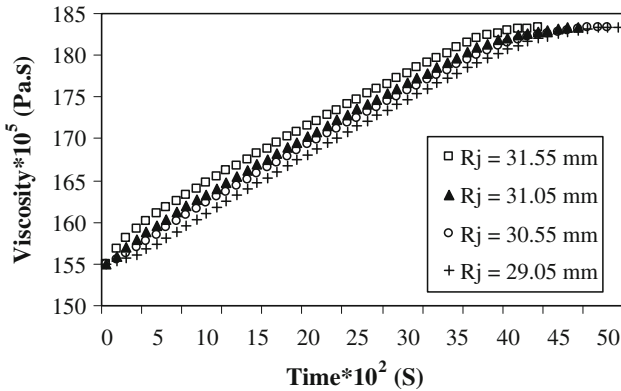


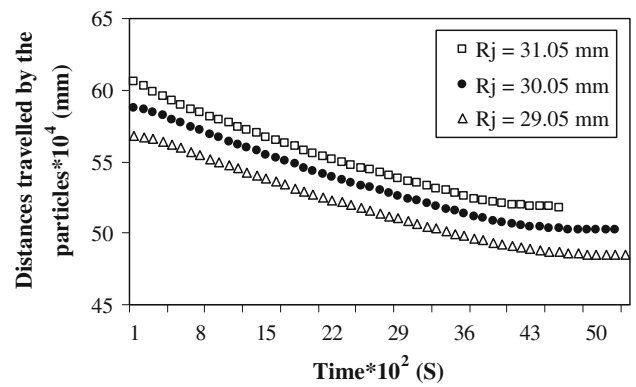
Fig. 5 Variation in viscosity as a function of time and position through the matrix ($T_{\text{metal,in}} = 700\text{ }^{\circ}\text{C}$, $T_{\text{mold,in}} = 400\text{ }^{\circ}\text{C}$)

Figure 5 which shows the viscosity variation as a function of time and position were generated based on the viscosity value at each time interval (Fig. 12 in Appendix 1). It can be seen from the figure that the viscosity increases with time as well as with position when moving from the inner to the outer casting face. The variation of the viscosity with the cooling time was calculated as the temperature was dropping to liquidus, as a minimum threshold. Thus, the metal was still in the liquid state. When the temperature of the metal drops below liquidus, the first solidification nucleus starts to form, making the movement of the particles difficult, and greatly increasing the viscosity of the metal.

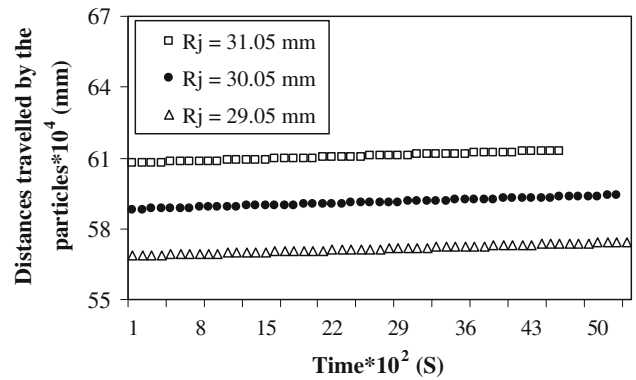
5.2 Distance Travelled by the Particles

Figure 6(a) and (b) which shows the distance travelled by the particles were generated based on the values of constant distances travelled by the particle at each time interval.

It can be seen (Fig. 6a) that when the variation of the viscosity with time and position is taken into account, the distances travelled by the particles decrease with time to reach a minimum value at a given time and position when the metal temperature approaches liquidus and the viscosity sharply increases. On the other hand, when the viscosity is constant (Fig. 6b), the distances travelled by the particles increase linearly with time before the particle is trapped by the liquid front. Moreover, the particles move at variable distances, depending on their original positions across the casting section. The decrease or the increase in the distances travelled by the



(a) Variable viscosity



(b) Constant viscosity

Fig. 6 Distances travelled by the particles as a function of time and position through the matrix ($T_{\text{metal,in}} = 700\text{ }^{\circ}\text{C}$, $T_{\text{mold,in}} = 400\text{ }^{\circ}\text{C}$)

particles influences their degrees of graduation through the section and affects their volume fraction on the outer casting face.

5.3 Theoretical and Experimental Results: Segregation of Particles

5.3.1 Influence of the Time Increment Variation. In our modeling, the discretization of the particle velocity which is expressed by the Stokes' law is done over time. The choice of Δt can influence the estimation of the particles' velocities during their segregation, the estimation of the total time of superheat extraction and the estimation of the particles' displacement during the cooling process.

In reality, the particle decelerates continuously. On one hand, the decrease in Δt , i.e., in the time interval produces a displacement of the particle closest to what is happening in reality. On the other hand, this decrease reduces the gap between the liquidus and the final value of temperature before it falls within the mushy zone. Therefore, it can be observed by comparing Fig. 7 with Fig. 8 that the distribution of particles and their volume fraction through the casting section becomes more homogeneous with decreasing Δt . The decrease in the particles' volume fraction on the outer casting face with increasing the time increment (Fig. 7) is explained by the large increment of time during the modeling that did not allow the temperature to reach a value close to the liquidus before falling below it. Therefore, the total time period, during which the particle moves decreases producing a decrease in the traveled

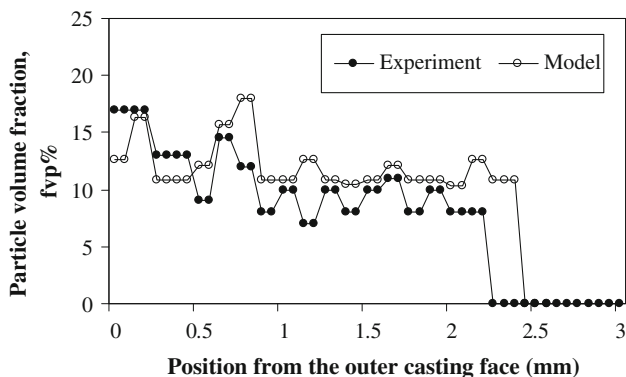


Fig. 7 Particle volume fraction variation for a time increment $\Delta t = 0.2$ s ($T_{\text{metal,in}} = 680$ °C, $T_{\text{mold,in}} = 350$ °C)

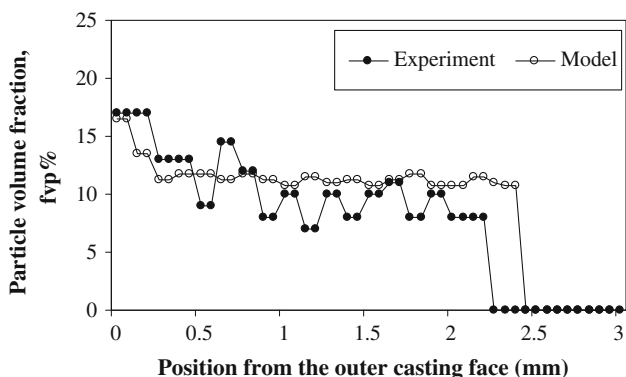


Fig. 8 Particle volume fraction variation for a time increment $\Delta t = 0.005$ s ($T_{\text{metal,in}} = 680$ °C, $T_{\text{mold,in}} = 350$ °C)

distance and volume fraction of particles on the outer casting face. Furthermore, it can be observed (Fig. 7) that the use of a large time increment can generate a less homogeneous volume fraction of particles across the section. This is explained by the sudden interruption of the particles' movement at various positions across the section at time (t_i). This interruption is due to the drop in temperature below the liquidus at time ($t_i + \Delta t$) without reaching a value close to the latter at time (t_i), given that during the modeling, the final considered value of the temperature is the one found above the liquidus depending on the used time increment. For a large Δt , the gap between the last variation of the temperature above the liquidus and the liquidus is greater than that when Δt is small. Thus, when the time increment is small, the particles can move until the temperature reaches a value closer to the liquidus before falling below it. Doing so allows particles to distribute more uniformly without being abruptly interrupted at different positions and different temperatures far from the liquidus before the solidification begins.

On the other hand, the concentration of the particles obtained experimentally across the section can be increased or decreased at different positions. This phenomenon is due to the formation of the primary phase which tends during its growth to push the particles to the interdendritic regions causing a heterogeneous variation in their concentration.

Figure 9 shows the variation in the particle volume fraction (fv) on the outer casting face as a function of Δt . In this figure, the variation of fv decreases and tends to reach a constant value

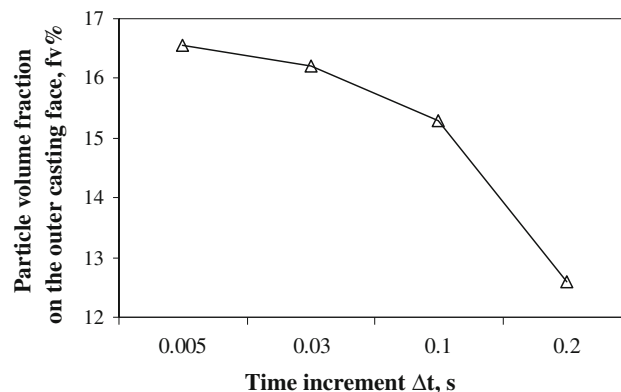


Fig. 9 Variation of the particles' volume fraction as a function of time increment ($T_{\text{metal}} = 680$ °C, $T_{\text{mold}} = 350$ °C)

Table 7 Modeling and experimental results of the particle volume fraction (fv) on the outer casting face without taking into account the influence of fv variation on particle segregation

Particle volume fraction, fv Position: 0.1 mm from the outer casting face					
Modeling results					
Initial temperature, °C	Metal	Mold	fv (constant viscosity	fv (variable viscosity	Experimental results, fv
			as a function of temperature)	as a function of temperature)	
700	700	100	19	14.5	15
700	700	400	22.5	19.8	18
680	680	350	20	16.5	17
650	650	30	10.4	10.4	11

with decreasing Δt . According to Fig. 9, the change in the volume fraction of particles as a function of Δt becomes less sensitive on the outer casting face when the time increment Δt becomes smaller. This can be explained by the high cooling rate on this face, which reduces at a certain time the effect of small decrease in the time increment on the displacement and volume fraction of the particles before they become blocked by the liquid front. Moreover, the decrease in Δt below 0.005 s will not change significantly the particles' volume fraction on the outer casting face (Fig. 9). The reduction in Δt improves the homogeneity of the particles' distribution and reduces the difference between the theoretical and the experimental results on the outer casting face.

5.3.2 Influence of Viscosity Variation with Temperature.

Table 7 shows the change in the particle volume fraction on the outer face of the composite for different initial molds and pouring temperatures, and with variable and constant viscosities.

The results show the impact of the variation in viscosity on the particle volume fraction. Modeling the particle volume fraction with a variable viscosity, while taking into consideration the change in the centrifugal radius during particle displacement, gives results that are closer to those obtained by experiments. In contrast, modeling using a constant viscosity

corresponding to the initial pouring temperature taking into account the initial particle volume fraction, gives higher particle volume fraction on the outer casting face compared to that obtained experimentally (Table 7). Furthermore, it may be noted, for the initial mold and pouring temperatures ($T_{\text{metal}} = 700\text{ }^{\circ}\text{C}$, $T_{\text{mold}} = 100\text{ }^{\circ}\text{C}$) and rotation speed used, that the particle volume fraction on the outer casting face does not reach a high value ($\approx 15\%V$).

Modeling the particle volume fraction with a constant viscosity, leads to a higher volume fraction of the particles on the outer casting face (Table 7). This is due to the higher distances travelled by the particles and to the accelerations that they undergo when only the change in the centrifugal radius is considered, while the particles move with decelerations if a variation of the viscosity with temperature is taken into account. Furthermore, the increase in the initial mold temperature leads to an increase in the volume fraction of particles on the outer casting face whether the modeling is done with a variable or constant viscosity (Table 7). On the other hand, with low initial mold and pouring temperatures ($T_{\text{metal}} = 650\text{ }^{\circ}\text{C}$, $T_{\text{mold}} = 30\text{ }^{\circ}\text{C}$), the volume fraction of the particles on the outer casting face is low and close to the initial particle volume fraction in the matrix (Table 7). When the difference between the initial pouring temperatures and the liquidus is small, and the initial temperature of the mold is low, the required time for superheat extraction, during which the viscosity undergoes a change, is decreased. Consequently, the change in the initial viscosity does not generate a big impact on the displacement of particles before the solidification begins. The cooling time at these temperatures is small, which does not allow the particles to move across a large distance before the solidification begins.

5.3.3 Influence of Viscosity Variation with Particle Volume Fraction. In our analysis, the influence of the initial particle volume fraction on the viscosity, and thereafter on the particle velocity and deceleration, was taken into account. On the other hand, as a first step, in order to even more clearly show the influence of the temperature change alone on the viscosity variation and particle velocity and segregation, the influence of the change in the particle volume fraction on viscosity and particle segregation, during centrifugation, was not considered. This allowed us to clarify the influence of the increase in viscosity on the particle velocity and segregation due to the decrease in the temperature alone without it being

Table 8 Modeling and experimental results of the particle volume fraction (fv) on the outer casting face while taking into account the influence of fv variation on particle segregation

		Particle volume fraction, fv Position: 0.1 mm from the outer casting face		
		Modeling results		Experimental results, fv
Initial temperature, $^{\circ}\text{C}$		fv (constant viscosity as a function of temperature)	fv (variable viscosity as a function of Temperature)	
Metal	Mold			
700	100	18.3	14	15
700	400	21.8	19	18
680	350	19.6	16	17

influenced by other phenomena, such as changes in the particle volume fraction. Thereafter, based on Eq 22, the particle segregation was recalculated after considering the influence of the variation in the particle volume fraction as a function of time and position on the apparent melt viscosity and particle velocity (Table 8).

In comparing the results of Table 8 with those of Table 7, which do not consider the influence of the variation in the particle volume fraction on the apparent melt viscosity and particle segregation, a small decrease in the particle volume fraction on the outer casting face due to the increase in the particle volume fraction and apparent melt viscosity on this face was observed.

On the other hand, the particle volume fraction on the outer casting face for the low initial mold and pouring temperatures ($T_{\text{metal}} = 650\text{ }^{\circ}\text{C}$, $T_{\text{mold}} = 30\text{ }^{\circ}\text{C}$), while taking into account the influence of the particle volume fraction variation on the apparent melt viscosity, is not supposed to undergo a significant variation because of the negligible increase of the particle volume fraction on this face while considering the change of the viscosity with temperature only (Table 7). However, the variation in the particle volume fraction during the centrifugation process would have a more remarkable influence on the apparent melt viscosity and particle segregation if the time of superheat extraction and the change of the particle volume fraction were greater than the results obtained in this study.

According to our results, the difference between the experimental and the theoretical results on the outer casting face, at a constant viscosity, varied from about 15 to 25%V depending on the initial pouring and mold temperatures, while this difference varied from about 2 to 5%V with variables viscosity and particle velocity. Thus, using variable viscosity in modeling gives more accurate results that are very consistent with experimental data.

6. Microstructure and Distribution of Particles

Figure 10 shows the segregation of particles at different locations from the external casting face. It can be seen from this figure that the volume fraction of particles decreases when advancing toward the inner face of the casting. Furthermore, Fig. 11 taken with optical microscope shows the variation in the microstructure across the casting section. The dendrite size increases while advancing to the inner casting face. In fact, the solidification speed at the inner casting face is lower when compared to that at the outer face which is in contact with the mold. The decrease of the solidification speed affects the formation of the primary phase. The lower the solidification speed the larger the dendrite size. The results agree with those of Rodriguez-Castro and Kelestemur (Ref 12).

7. Discussions

The main interest of our work lies in its allowing us, when modeling the segregation of particles, to consider the evolution of the viscosity with temperature and cooling rate across the matrix, in addition to the change of the centrifugal radius during the displacement of the particle. This allows for a precise prediction of the volume fraction of the particles on the outer

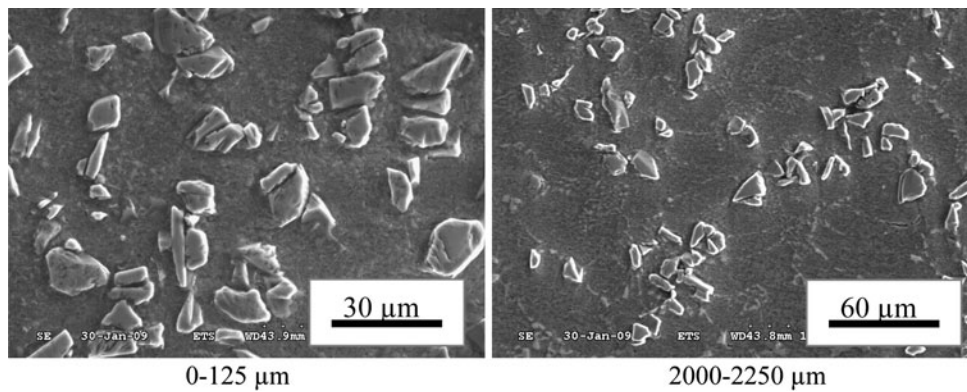


Fig. 10 Segregation of particles, $T_{\text{metal,in}} = 700\text{ }^{\circ}\text{C}$, $T_{\text{mold,in}} = 400\text{ }^{\circ}\text{C}$ (distances taken from the outer casting face)

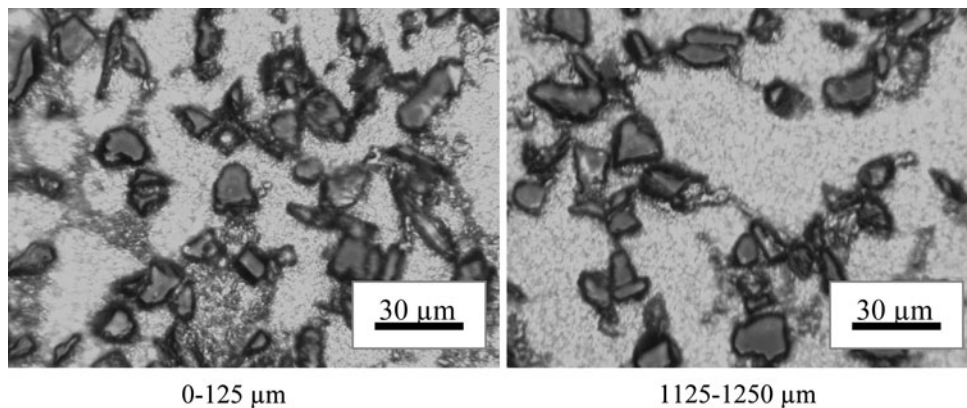


Fig. 11 Microstructures of Al/SiC composite (distances taken from the outer casting face)

casting periphery. Furthermore, this work modeled the real variation in the particle velocity and deceleration during the centrifugation process, using Stokes' law at each discrete time interval for a particle moving at a constant velocity. The analysis done in this work illustrates the impact of the change in the centrifugal radius with the displacement of the particle and the increase in the viscosity with the decrease in temperature, on the dynamic and behavior of particles during their segregation.

It was found in this work, while taking into account the variation of the centrifugal radius during centrifugation process that changes in the melt viscosity during the cooling process can have a significant impact on particle segregation and volume fraction on the outer casting face, depending on the initial pouring and mold temperatures and on the process parameters. Modeling of the velocity, deceleration/acceleration, displacement, and volume fraction of the particles, taking into account the change in temperature, cooling rate, and centrifugal radius, shows the effect of the variation in the viscosity on the segregation of the particles, and leads to results which better match their experimental counterparts on the outer casting face. In contrast, modeling particle segregation with a constant viscosity can lead to a higher volume fraction on the outer casting face than that obtained experimentally. Furthermore, the higher the initial pouring and mold temperatures, the higher the effect of the viscosity variation. This is explained by the increase of the cooling time. The higher the time required to

extract superheat, the higher the effect of the viscosity on the segregation of the particles. The volume fraction of the particles on the outer casting face stops increasing when the solidification begins. This analysis is in line with the results found by Lajoie and Suery (Ref 6), who show that when the solidification of liquid metal begins very quickly, with no superheat to extract, the volume fraction of the particles on the outer face of Al/SiC composite is low and very close to that obtained at the beginning of the segregation zone near the inner face. Moreover, for large particles' volume fraction, interaction between particles occurs, thus reducing the particles' velocity. According to Lajoie and Suery (Ref 6) and Raju and Mehrotra (Ref 3), it is assumed that the reduction in velocity due to the particles' interactions is characterized by an increase of the liquid's apparent viscosity. Thus, the influence of particles' interaction on particle velocity is considered with the change in apparent melt viscosity.

The volume fraction of the particles on the outer casting face and through the matrix should be controlled taking into account the impact of the cooling rate and the variation of the centrifugal radius and melt viscosity with time and position. The fact that the increase in the initial pouring and mold temperatures increases the required time for the extraction of superheat allows particles to move across larger distances. Consequently, their volume fraction on the outer face becomes higher. On the other hand, the value of the time increment used

in the modeling affects the particles' segregation. A large time increment causes a heterogeneous distribution of particles across the casting section and reduces their volume fraction on the outer face because of the reduction of the total time of cooling used in the modeling. In contrast, the reduction in the time increment improves temperature distribution across the section and increases the displacement time of the particles. Consequently, the particles distribute more homogeneously and their volume fraction on the outer casting face becomes closer to that obtained experimentally.

In order to analyze the influence of the change of the particle volume fraction on the temperature and cooling rate variation across the casting section, an analysis of heat transfer was done using FLUENT with different particle volume fractions ($f_v = 10\%$, $f_v = 20\%$) and given initial pouring and mold temperatures ($T_{\text{metal}} = 700\text{ }^\circ\text{C}$, $T_{\text{mold}} = 400\text{ }^\circ\text{C}$). The results show that the maximal difference in the cooling rate between the different particle volume fractions used is about $0.617\text{ }^\circ\text{C/s}$, which corresponds to a variation in temperature and cooling time of $0.35\text{ }^\circ\text{C}$ and 0.002 s , respectively, for a total time of cooling of 0.57 s . Thus, the time of superheat extraction during which the particles move is almost the same whether the particle volume fraction was 10 or 20%V, and the variation in the cooling rate and temperature is insignificant. Consequently, we assume, for the parameters and experimental conditions used in our study that the increase in the particle volume fraction to $f_v = 20\%V$ on the outer casting face, does not affect significantly the temperature variation and particles' displacement and segregation during the extraction of superheat.

8. Conclusions

- In this work, variations in the centrifugal radius during the segregation of the particles are combined with the change in viscosity during the cooling process. It was found that the particle behavior varies with time and position whether the used centrifugal radius, viscosity, and therefore velocity of the particle are constants or variables.
- A significant effect of melt viscosity variation and centrifugal radius change on particle segregation during the centrifugation process is shown in this study. Modeling the particles' volume fraction variation with a variable viscosity as a function of temperature produces results that are more accurate and closer to those obtained experimentally on the outer casting face.
- Increasing the initial mold and pouring temperatures accentuates the effect of viscosity on particle segregation and increases the time required to extract superheat. This would favor a higher volume fraction of particles on the outer casting face. On the other hand, according to the parameters and conditions used in this work, and for low initial pouring and mold temperatures, the volume fraction of the particles on the outer casting face is low and almost similar to the initial particle volume fraction in the matrix.
- The reduction in the time increment increases the homogeneity of the particles' distribution. Moreover, the particles' volume fraction on the outer face comes closer to the results obtained experimentally.

Appendix 1

See Fig. 12 to 14.

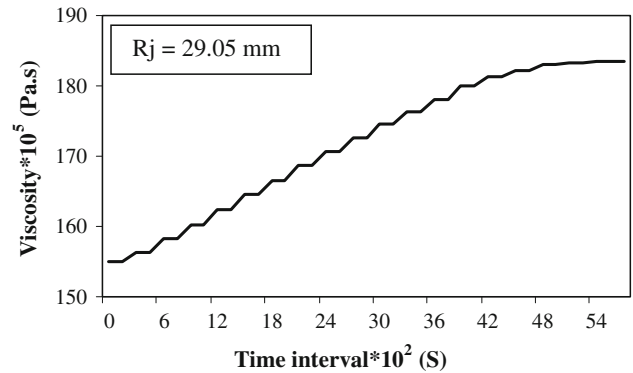


Fig. 12 Viscosity of liquid metal as a function of time interval ($\Delta t = 0.03\text{ s}$) ($T_{\text{metal,in}} = 700\text{ }^\circ\text{C}$, $T_{\text{mold,in}} = 400\text{ }^\circ\text{C}$)

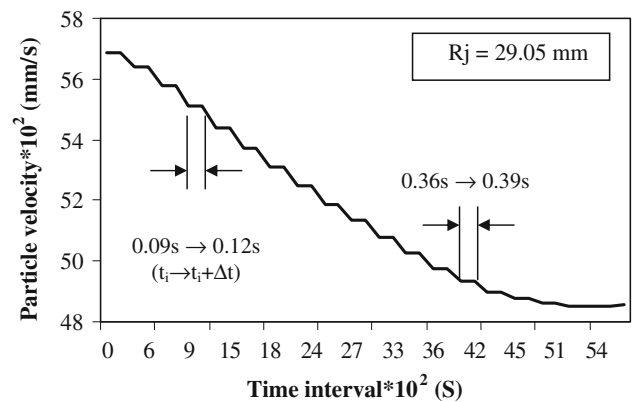


Fig. 13 Constant particle velocity as a function of time interval ($\Delta t = 0.03\text{ s}$) ($T_{\text{metal,in}} = 700\text{ }^\circ\text{C}$, $T_{\text{mold,in}} = 400\text{ }^\circ\text{C}$)

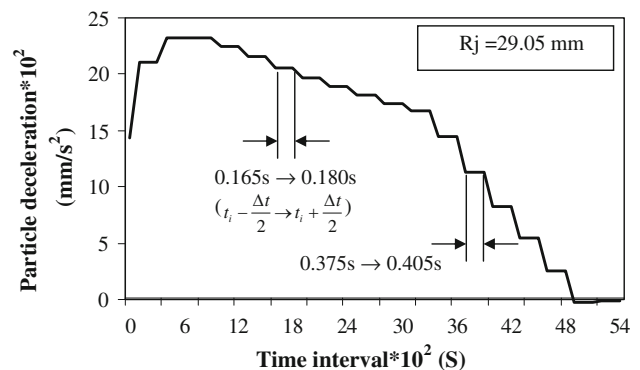


Fig. 14 Constant particle deceleration as a function of time interval ($\Delta t = 0.03\text{ s}$) ($T_{\text{metal,in}} = 700\text{ }^\circ\text{C}$, $T_{\text{mold,in}} = 400\text{ }^\circ\text{C}$)

References

1. Y. Watanabe, N. Yamanaka, and Y. Fukui, Control of Composition Gradient in a Metal-Ceramic Functionally Graded Material Manufactured by the Centrifugal Method, *Composites A*, 1998, **29A**, p 595–601
2. F. Bonollo, A. Moret, S. Gallo, and C. Mus, Cylinder Liners in Aluminum Matrix Composite by Centrifugal Casting, *Metall. Italiana*, 2004, **96**, p 49–55
3. P.S.S. Raju and S.P. Mehrotra, Mathematical Modeling of Centrifugal Casting of Metal Matrix Composites, *Mater. Trans. JIM*, 2000, **41**, p 1626–1635
4. A. Velhinho, P.D. Sequeira, F. Braz Fernandes, J.D. Botas, and L.A. Rocha, Al/SiCp Functionally Graded Metal-Matrix Composites Produced, by Centrifugal Casting: Effect of Particle Grain Size on Reinforcement Distribution, *Presented at Proceedings of the Seventh International Symposium on Functionally Graded Materials*, Oct 15–18 2002, Beijing, China, 423–425, 2003, p 257–262
5. M.F. Forster, R.W. Hamilton, R.J. Dashwood, and P.D. Lee, Centrifugal Casting of Aluminium Containing In Situ Formed TiB, *Mater. Sci. Technol.*, 2003, **19**, p 1215–1219
6. L. Lajoie and M. Suery, Modelling of Particle Segregation During Centrifugal Casting of Al-Matrix Composites, *Proceedings of the International Symposium on Advances in Cast Reinforced Metal Composites*, Sep 26–30, Chicago, IL, 1988, p 15–20
7. E. Panda, D. Mazumdar, and S.P. Mehrotra, Mathematical Modeling of Particle Segregation During Centrifugal Casting of Metal Matrix Composites, *Metall. Mater. Trans. A*, 2006, **37**, p 1675–1687
8. D.R. Poirier and E.J. Poirier, *Heat Transfer Fundamentals for Metal Casting*, TMS, Warrendale, PA, 1991, p 1–59
9. A. Grabowski, M. Nowak, and J. Sleziona, Optical and Conductive Properties of AlSi-Alloy/SiC Composites: Application in Modelling CO₂ Laser Processing of Composites, *Opt. Lasers Eng.*, 2005, **43**, p 233–246
10. D.M. Stefanescu, A. Moitra, A.S. Kacar, and B.K. Dhindaw, Influence of Buoyant Forces and Volume Fraction of Particles on the Particle Pushing/Entrapment Transition During Directional Solidification of Al/SiC and Al/Graphite Composites, *Metall. Trans. A*, 1990, **21A**, p 231–239
11. Fluent 6.2 documentation, [L:/fluent.inc/help/index.htm](http://fluent.inc/help/index.htm)
12. R. Rodriguez-Castro and M.H. Kelestemur, Processing and Microstructural Characterization of Functionally Gradient Al A359/SiCp Composite, *J. Mater. Sci.*, 2002, **37**, p 1813–1821